Energy confinement of high-density tokamaks

Energy Confinement of High-Density Tokamaks

F. C. SCHULLER AND D. C. SCHRAM*
Association Euratom-FOM, FOM-Instituut voor Plasmafysica
Rijnhuizen, Jutphaas, The Netherlands
(*Technical University, Eindhoven)

ABSTRACT

It will be proven that neoclassical ion heat conduction is the major energy loss mechanism in the centre of an ohmically heated high-density tokamak discharge ($n > 3 \times 10^{20}$ m^{-3}). This fixes the mutual dependence of plasma quantities on axis and leads to scaling laws for the poloidal beta and energy confinement time given the empirical fact that the pressure profile and the current-density profile are Gaussians.

I. INTRODUCTION

Gas-puffing techniques have made it possible to raise the density by one to two orders of magnitude during a tokamak discharge. The Alcator team [1,2,3] reported on an electron density rise from 10^{19} to 10^{21} m^{-3}. It was noticed that β_θ and τ_E went up proportionally to n and the ion temperature increased from 150 eV to 800 eV, i.e., to a value equal to the electron temperature T_e.

It is known that at low density anomalous electron heat conduction is the major loss mechanism. The ohmic power input stays constant with increasing density. This means that the anomalous electron heat conduction is independent of the density or even diminishes with the density because other loss mechanisms increase with the density. Plateau ion heat conduction increases proportionally to $n_i T_i^{5/2}$. *Now the question arises: at which density does the plateau ion heat conduction develop into the major loss mechanism*? The answer to this question cannot be found by comparing the experimental energy-confinement time with theoretical values because these calculations are approximations, not taking the profiles correctly into account. Comparison with the results of numerical codes is possible, but the codes have too many "knobs" that can be adjusted. Moreover, they cannot easily reach the highest experimental densities because the mechanism responsible for the inward transport of plasma is still unknown.

A simple method for analyzing the energy balance, which will be described here, is based on an empirical approach:

- how large is the experimental heat flow as a function of the radius, calculated from the radial dependence of the ohmic power input;
- how large is the heat flow due to ion heat conduction as calculated from the experimental temperature and density profiles, disregarding the question how these profiles could have been developed in the history of the discharge;
- at what density and which radius does the empirical heat flow become comparable to the ion heat conduction flow?

This method is described extensively elsewhere [4].

II. DESCRIPTION OF THE METHOD

1. The experimental laser-scattering data n_e^{exp} and T_e^{exp} must be fitted with Gaussians such that one-dimensional profiles can be derived of the form:

$$T_e(r) = T_{eo} \exp\left[-r^2/\Lambda_T^2\right]. \tag{1a}$$

$$n_e(r) = n_{eo} \exp\left[-r^2/\Lambda_n^2\right]. \tag{1b}$$

An Alcator discharge as described by Apgar et al. [2] will be taken as a reference discharge. Laser scattering data were measured at a point in time when the density was highest and constant ($\partial n/\partial t = 0$) and also the discharge current was constant ($\partial I/\partial t = 0$):

$$R = 0.54 \text{ m}\,; \quad B_T = 7.1 \text{ T}\,; \quad n_{eo} = 6 \times 10^{20} \text{ m}^{-3}\,; \quad \Lambda_n = 0.07 \text{ m}\,;$$

$$a = 0.095 \text{ m}\,; \quad I_T = 0.108 \text{ MA}\,; \quad T_{eo} = 0.77 \text{ keV}; \quad \Lambda_T = 0.05 \text{ m}\,.$$

The experimental laser-scattering data and the Gaussians used for determining the one-dimensional profiles are shown (Fig. 1).

2. The assumption that Z_{eff} is constant over the radius and that corrections for trapped electrons are negligibly small, leads to a straightforward expression for the current-density profile:

$$j(\alpha T_e^{3/2}) = j_o \exp\left[-r^2/\Lambda_c^2\right] \quad \text{with} \quad \Lambda_c = \Lambda_T \sqrt{2/3}\,. \tag{2}$$

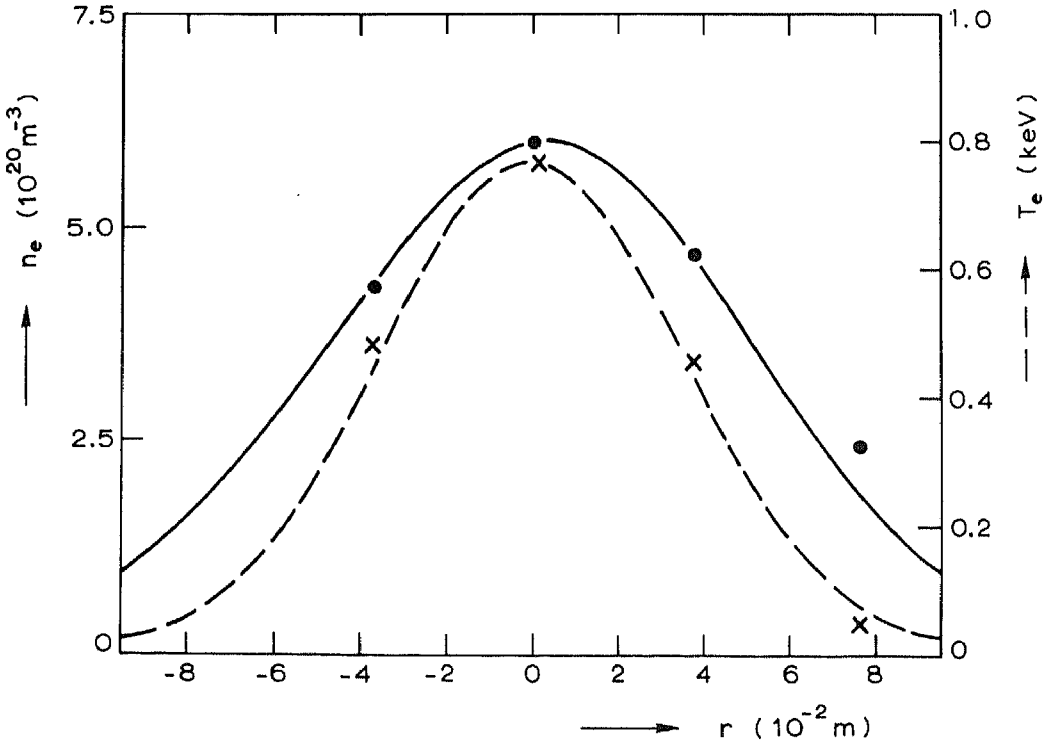

FIGURE 1. *Electron temperature and density profiles of the reference Alcator discharge [2] with the approximation by Gaussians characterized by* $\Lambda_T = 0.05$ *m, displacement* $\Delta_T = -1 \times 10^{-3}$ *m and* $\Lambda_n = 0.07$ *m,* $\Delta_n = +4 \times 10^{-3}$ *m.*

The correctness of this expression can be judged by calculating the values for q_o and Z_{eff}, which are consistent with this current-density profile. For our reference discharge we find: $q_o = 1.0$ and $Z_{\text{eff}} = 1.14$. Terry et al. [5] have determined Z_{eff} for the same discharge with ultraviolet spectroscopy. Their result is: $Z_{\text{eff}} = 1.16$.

3. The empirical heat flow, $Q^{\text{eff}}(r)$, can now easily be calculated from:

$$Q^{\text{eff}}(r) = \frac{V_\ell}{2\pi r R}\int_0^r j(r')r'\,dr' = 2.5\times 10^4\,\frac{V_\ell \hat{I}}{R\Lambda_c G_c}\left\{\frac{\Lambda_c}{r}\left(1-\exp\left[-r^2/\Lambda_c{}^2\right]\right)\right\}\quad \text{W/m}^2 \tag{3}$$

in which V_ℓ is the loop voltage corrected for inductive effects, $\hat{I}$ is the current in MA, and $G_c = (1 - \exp[-a^2/\Lambda_c{}^2])$.

4. The heat flow due to ion heat conduction, $Q_i^{\text{cond}}(r)$, is given by:

$$Q_i^{\text{cond}}(r) = -\kappa_i\,\frac{\partial T_i}{\partial r} = -C_{22}^i\,\sqrt{2}\,\frac{n_i k T_i}{m_i \omega_{ci}^2 \tau_{ii}}\,\frac{\partial k T_i}{\partial r}, \tag{4}$$

in which τ_{ii} is the ion-ion collision time and ω_{ci} the ion gyro-frequency. The neoclassical enhancement factor C_{22}^i depends on the collisionalities ν^* and ν^{**}:

$$\nu^* = (R/r)^{3/2}\nu^{**} = (R/r)^{3/2}\,\frac{q(r)R_o}{V_{thi}(r)\tau_{ii}(r)}; \tag{5}$$

banana and plateau diffusion, $\nu^{**} < 1$ (Rutherford et al. [6]):

$$C_{22}^i = 2q^2(R/r)^{3/2}\,\frac{0.48}{1 + 0.36\nu^*} \qquad \text{NC} \tag{6a}$$

for Pfirsch-Schlüter diffusion $\nu^{**} > 1$:

$$C_{22}^i = 2.26\,q^2 \qquad \text{PS} \tag{6b}$$

All three regimes (Hazeltine, Hinton [7]):

$$C_{22}^i = 2q^2\,0.47(R/r)^{3/2}\,\frac{1 + 0.43\nu^{**}}{1 + 1.03(\nu_i^*)^{1/2} + 0.18\nu^*}. \qquad \text{HH} \tag{6c}$$

5. Necessary for the calculation of Q_i^{cond} are the values of the quantities $n_i(r)$, $q(r)$ and $T_i(r)$. For our reference discharge Z_{eff} is so close to unity that $n_i \sim n_e$; $q(r)$ can be calculated from $j(r)$. The problem is to find $T_i(r)$ since charge-exchange neutral analysis fails due to the opaqueness of the high-density plasmas for neutrals.

One can calculate the *lowest* possible T_i from the assumption that all the ohmic power input is transferred from the electrons to the ions:

$$T_i^{\min} = T_e\left(1 - \frac{\tau_{\text{coul}}}{\tau_{Ee}}\right). \tag{7}$$

In this equation τ_{coul} represents the energy transfer time due to collisions between electrons and ions and τ_{Ee} the experimental energy confinement time of the electrons. The calculation for the reference discharge gives:

$$T_{io}^{\min} = 0.88\, T_{eo} \qquad \text{on axis;}$$

$$\langle T_i^{\min} \rangle = 0.095\, \langle T_e \rangle \quad \text{averaged over the radius.}$$

For the calculations we now start with the *trial* assumption:

$$T_i(r) \simeq 0.93\, T_e(r)\,. \tag{8}$$

6. The calculations of Q_{NC}^{cond}, Q_{PS}^{cond} and Q_{HH}^{cond} can be done with the trial assumption of Eq. (8). If ion heat conduction is the only energy loss mechanism, the ratio Q^{cond}/Q^{eff} must be equal to one.

The result (Fig. 2) shows that Q^{cond}/Q^{eff} is even larger than one. This inconsistency is caused by the trial assumption for T_i. In reality the T_i-profile is flatter in the centre and somewhat steeper at the outside since the coupling between ion and electron temperature is weakest on axis. Examination of the ν^* value in the central region indicates that for $r \leqslant \Lambda_c$ the ions are in the plateau regime. A more realistic T_i-profile can be calculated by assuming that the ratio Q^{cond}/Q^{eff} is constant and has the value C_Q. Integration of the assumed equality:

$$\frac{\partial T_i}{\partial r} = -C_Q \frac{Q^{eff}}{\kappa_{plat}} \tag{9}$$

leads to the T_i-profile:

$$\hat{T}_i(r)^* = \left\{ \hat{T}_{io}^{*5/2} - 0.064 \frac{BR\hat{I}^2 V_\ell C_Q}{\hat{n}_{eo} G_c^{\,2}} \int_0^r \exp\left[r'^2/\Lambda_n^{\,2}\right] \frac{\left[1 - \exp\left(-r'^2/\Lambda_c^{\,2}\right)\right]^2}{r'^3}\, dr \right\}^{2/5} \tag{10}$$

in which $\hat{T}_i$ is expressed in keV, $\hat{n}$ the density is expressed in 10^{20} m^{-3}, $\hat{I}$ the current in MA. If one assumes that the part of the ohmic power, that is not lost by ion heat conduction, is lost through the electron channel, one can easily calculate the "ansatz" for the temperature on axis, T_{io}^*, by adapting Eq. (7):

$$T_{io}^* = T_{eo}\left[1 - C_Q \frac{\tau_{coul}}{\tau_{Ee}}\right]. \tag{11}$$

7. The resulting T_i^*-profiles are presented in Fig. 3. Curve *a* represents the Gaussian T_e-profile reduced to one dimension; curve *b* shows the trial profile $T_i = 0.93\, T_e$, which leads to an inconsistent energy balance in the central region ($Q^{cond} > Q^{eff}$). The T_i^* profile for $C_Q = 0.5$ and 1 are given by curves *c* and *d* respectively. It is clear that $C_Q = 1$ gives the best result. All in all it can be concluded that:

a. $0.5 < Q^{cond}/Q^{eff} \simeq 1$ for $0 < r < \Lambda_c$.

b. $0.1 < Q^{cond}/Q^{eff} < 0.5$ for $\Lambda_c < r < 2.3\Lambda_c (= a)$. Estimates of other loss mechanism can be made (Table 1). From this table one can see that together with ion heat conduction the energy balance in the central region and at the very outside can be fully explained by classical processes, but:

c. In the region between $\Lambda_c < r < 2\Lambda_c$, there is a possibility of anomalous heat conductivity.

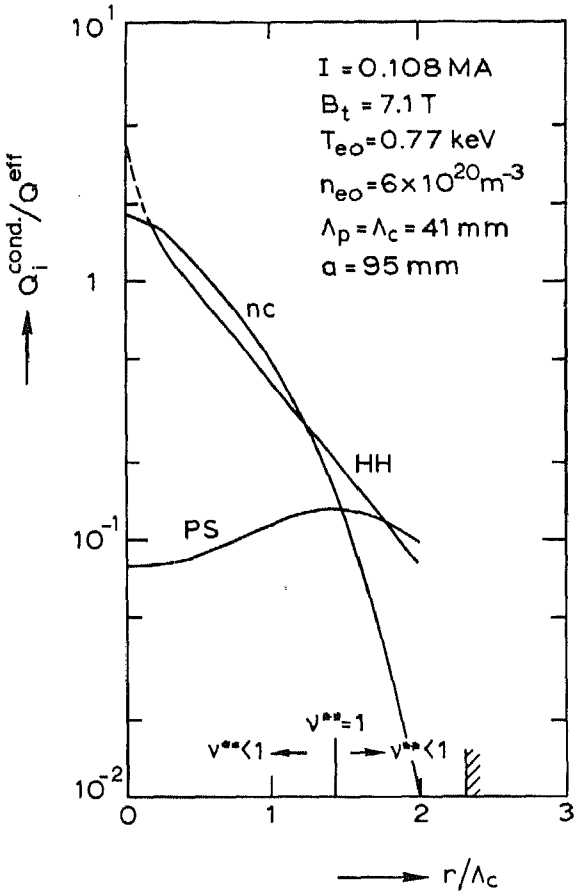

FIGURE 2. *The ratio* Q^{cond}/Q^{eff} *for neoclassical (NC), Pfirsch-Schlüter* (PS) *and Hazeltine-Hinton* (HH) *ion heat conduction as a function of the radius for the reference discharge in Alcator with trial function* $T_i = 0.93\ T_e$.

III. SEMI-EMPIRICAL SCALING LAWS FOR $\beta_{\theta e}$ AND τ_{Ee}

For our reference discharge the *empirical* fact is proven that the profiles of n_e, T_e, P_e and j can be described by Gaussians. The value of these quantities on axis is such that plateau ion heat conduction is the dominating energy loss. The halfwidth of the Gaussians is determined by other loss mechanisms. If one postulates that all discharges in the high-density regime can be described by some characteristics, i.e., Gaussian profiles with plateau ion heat conduction as the major loss mechanism on axis, one can derive semi-empirical scaling laws for T_e, $\beta_{\theta e}$ and τ_{Ee} as a function of n_e, B, I and geometry.

The quantities on axis must be interrelated by the requirement:

$$C_Q = Q_{\text{plat}}^{\text{cond}}/Q^{\text{eff}} = K\,\frac{A_i^{1/2}}{Z_{\text{eff}}Z_i^3}\,\hat{n}_{eo}\hat{T}_{eo}^4\left(\hat{T}_{io}/\hat{T}_{eo}\right)^{5/2}\,\frac{Rq_o^3}{\Lambda_c^2 B^4}. \tag{12}$$

The numerical factor K is necessary because the T_i-profile is not Gaussian. This is proven by the inconsistent value of $C_Q = 2$ for the Gaussian trial profile (Section II.6). The value of K can be calculated from the values of the reference discharge: $C_Q = 1.00 - 0.08 = 0.92$ (see Table 1); $T_{io}/T_{eo} = (1 - 0.92\ \tau_{\text{coul}}/\tau_{Ee}) = 0.89$; $\hat{n}_{eo} = 6$; $\hat{T}_{eo} = 0.77$; $Z_i = 1$; $Z_{\text{eff}} = 1.14$; $A_i = 1$; $q_o = 1$; $\Lambda_c = 0.041$ m; $B = 7.1\ T$. This leads to $K = 5.0$.

From Eq. (12) a scaling law for $\hat{T}_{eo}$ can be derived:

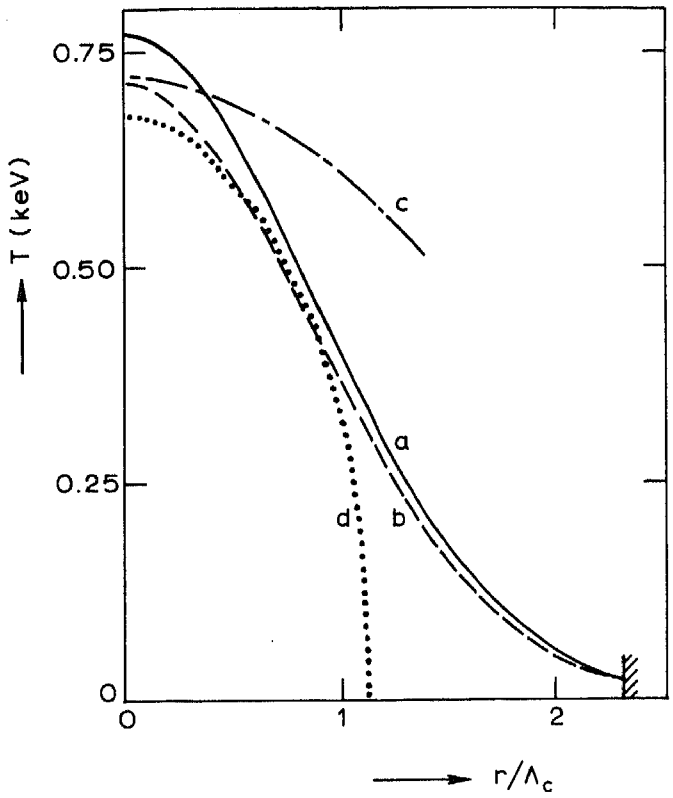

Figure 3. *One-dimensional temperature profiles of the reference discharge. Curve a: the experimental Gaussian electron-temperature profile; Curve b: the trial ion-temperature profile* $T_i = 0.93\ T_e$*; Curve c: the ion-temperature profile calculated for* $C_Q = 0.5$*; Curve d: the ion temperature profile calculated for* $C_Q = 1$.

Table 1

The estimated relative contribution of various loss mechanisms to the effective heat flow at various radii r:

Type	$r = 0$	$r = \Lambda_c$	$r = 1.5\ \Lambda_c$	$r = 2\Lambda_c$	$r = 2.3\Lambda_c = a$
Convection	—	0.05	0.11	0.22	0.33
Charge exchange	—	0.01	0.05	0.16	0.28
Bremstrahlung	0.01	0.01	0.01	0.01	0.01
Total neutral line radiation	—	—	—	0.01	0.04
Impurity line radiation for C_iN	0.02	0.03	0.04	0.06	0.07*
Line radiation for Mo	0.05	0.07	0.09	0.12	0.13*
	0.08	0.17	0.30	0.58	0.86

*Measurements of Terry et al. (5).

$$\hat{T}_{eo} \simeq 0.7\, C_Q^{1/2} Z_i A_i^{-1/8} \hat{n}_{eo}^{-1/4} B a^{1/4} (a/R)^{1/4} \left[(\hat{T}_{eo}/\hat{T}_{io})^{5/8} (\Lambda_c/a)^{1/2} q_o^{-3/4}\right]. \quad (13)$$

The factor between [ ]-brackets will not differ very much for various discharges since $T_{eo} \simeq T_{io}$; $\Lambda_c/a \sim (q_o/q(a))^{1/2}$; $q_o \simeq 1$ and $q(a)$ is bound to a lower limit for stable operation. The dependence on I comes in via $q(a)$. This value of $\hat{T}_{eo}$ can be used in the definition of $\beta_{\theta e}$:

$$\beta_{\theta e} \equiv \frac{2\mu_o}{B_p(a)^2} \int_0^r P_e 2\pi r'\, dr'/\pi a^2 = 4 \times 10^{-2} \hat{n}_{eo} \hat{T}_{eo} B^{-2} (R/a)^2 \left[q_o (a/\Lambda_c)^2 (\Lambda_p/\Lambda_c)^2\right]$$

$$= 2.8\, 10^{-2} C_Q^{1/4} Z_i A_i^{-1/8} \hat{n}_{eo}^{3/4} B^{-1} a^{1/4} (R/a)^{7/4} \left[(\hat{T}_{eo}/\hat{T}_{io})^{5/8} (a/\Lambda_c)^{3/2} q_o^{5/4} (\Lambda_p/\Lambda_c)^2\right], \quad (14)$$

in which $\Lambda_p = (1/\Lambda_n^2 + 1/\Lambda_T^2)^{-1/2}$.

In Fig. 4 the experimental $\beta_{\theta e} \cdot B$-values measured at various external parameters are plotted against $\hat{n}_{eo}$. The straight lines represent the scaling law of Eq. (14) with various values for the [ ]-factor equal to the value of the reference discharge. It can be noticed that for $n_{eo} > 3 \times 10^{20}$ m^{-3} the points follow the $C_Q = 1$ line. At lower densities loss mechanisms other than ion heat conduction are also important in the centre. This characteristic density will presumably have other values in other machines. One helium discharge in the ST-device with a $Z_{\text{eff}} \simeq Z_i = 2$, corrected for the different geometry and atomic numbers, Z_i and A_i, fits also the $C_Q = 1$ line.

In the same way a scaling law for τ_{Ee} can be derived:

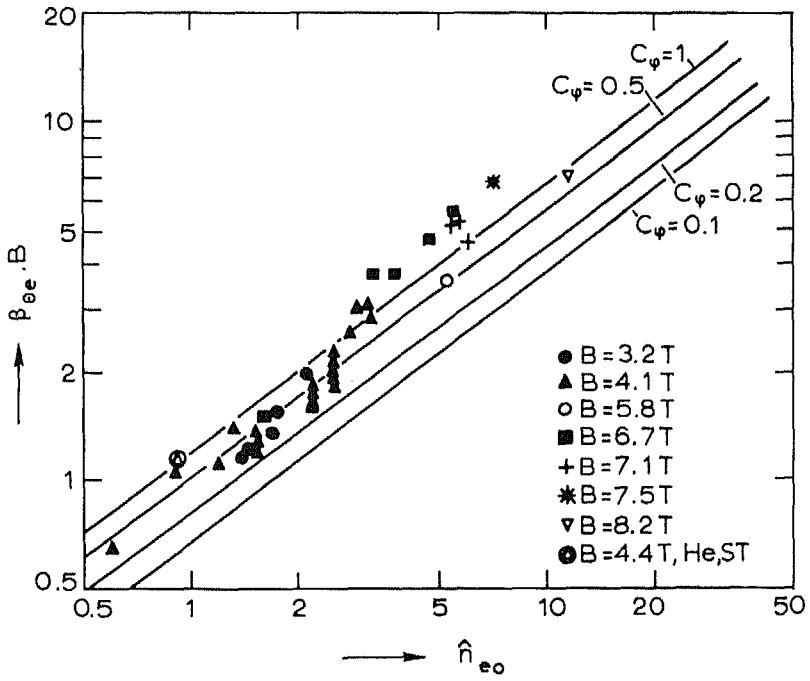

FIGURE 4. *The experimental product $\beta_{\theta e} \cdot B$ as a function of n_{eo} for Alcator discharges in H_2 at various magnetic fields as indicated. Ⓐ indicates an ST-discharge in He, scaled with Z_i and geometry; the $\beta_{\theta e} \cdot B$-values are calculated from Eq. (14) with: $\Lambda_c = \Lambda_p$; $T_{io} = 0.85\, T_{eo}$; $a/\Lambda = 2.3$ $(q(a) = 5.3)$; $R/a = 5.7$; $a = 0.095$ m; $q_o = 1$; with $C_\phi = 0.1$, 0.2, 0.5, and 1.0.*

$$\tau_{Ee} = \frac{4\pi^2 R}{IV}\int_0^a n_e k T_e r'\,dr' = 0.14 C_Q^{5/8} Z_i^{3/2} A_i^{-5/16} \hat{n}_{eo}^{3/8} B^{1/2} a^{21/8} (R/a)^{11/8} \times$$

$$\times \left[T_{eo}/T_{io}\right)^{25/16} (\Lambda_c/a)^{5/4} q_o^{1/8} (\Lambda_p/\Lambda_c)^2]\,. \qquad (15)$$

In Fig. 5 the experimental τ_{Ee}-values are plotted against $\hat{n}_{eo}^{3/8} B^{1/2}$. Straight lines represent the scaling law of Eq. (15) for $C_Q = 0.5$ and 1 and a fixed value of the [ ]-factor equal to the value of the reference discharge. Although the scatter in the experimental points is larger than in the $\beta_{\theta e}$-plot, the values are in agreement with $0.5 < C_Q < 1$.

Note 1. The scaling $\tau_E \propto n_e^{3/8} B^{1/2}$ is not in disagreement with the older scaling proposed by the Alcator team, i.e., $\tau_E \propto n$, since in the last one the influence of B is not taken into account. The maximum density which can be obtained is roughly proportional to B. Therefore, $\tau_E \propto n^{3/8} B^{1/2} \propto n_e^{7/8}$, which is undistinguishable from $\tau_E \propto n$.

Note 2. Connor and Taylor [8] have studied the general properties of scaling laws for τ_E as given by the fact that the basic transport equations (i.e., the Vlasov equation) are invariant under a certain group of transformations. For the low-β collisional case of an ohmically heated plasma they found:

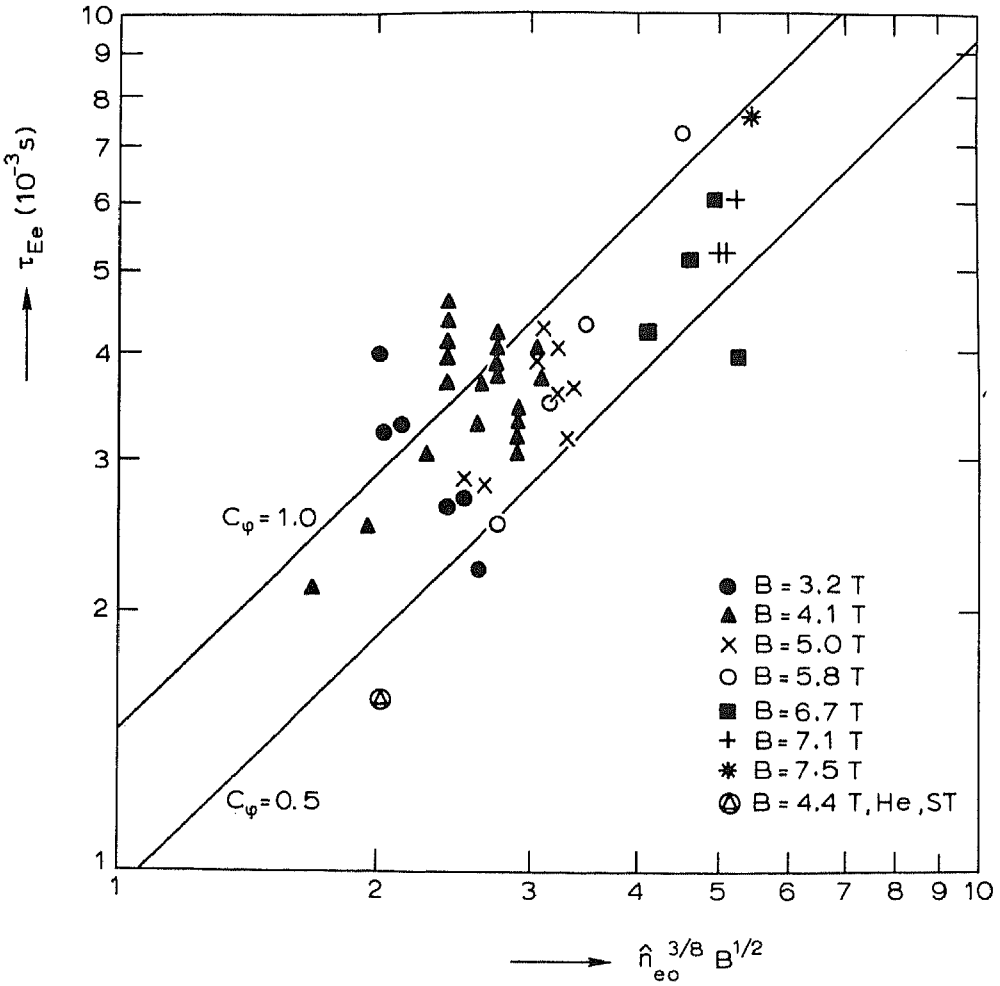

FIGURE 5. *The experimental electron energy confinement time τ_{Ee} as a function of $n_{eo}^{3/8} B^{1/2}$ for Alcator discharges at various magnetic fields are indicated. The τ_{Ee}-values are calculated with the half-empirical scaling law of Eq. (15) at the same parameters as in Fig. 4, with $C_Q = 0.5$ and 1.0.*

$$\tau_E = n_e^x B^{y-1} a^z,$$

in which the powers x, y and z have to meet the condition:

$$8x + 5y - 4z = 0.$$

Eq. (15) is in agreement with this condition.

Note 3. If one applies the scaling laws for the prediction of the performance of other ohmically heated high-magnetic field tokamaks, one finds for instance for the FT-device the following set of parameters:

$$R = 0.83\,\text{m};\quad a = 0.21\,\text{m};\quad B = 10\,\text{T};\quad I = 500\,\text{kA}\,(q_a = 5.3);$$
$$n_{eo} = 10^{21}\,\text{m}^{-3};\quad T_{eo} = 1.58\,\text{keV};\quad \beta_{\theta e} = 0.41;\quad \tau_{Ee} = 44\,\text{msec};$$
$$T_{io}/T_{eo} = 0.98.$$

IV. CONCLUSIONS

1. It was proven that neoclassical ion-heat conduction of the plateau regime is the major loss mechanism in the centre of Alcator discharges with a central density higher than 3×10^{20} m^{-3}. This characteristic density value depends on the relative importance of other loss mechanisms, especially anomalous electron heat conduction, the nature of which is unknown. Therefore, other tokamaks may have a different characteristic density value.

2. In the outside region of the discharge other loss mechanisms for the electrons as well as for the ions surpass the ion heat conduction of the Pfirsch-Schlüter regime. The most important ones are convection, charge-exchange losses and impurity line radiation. Anomalous heat conduction cannot be ruled out, but it cannot be larger than 50% at the most.

3. Semi-empirical scaling laws for T_{eo}, $\beta_{\theta e}$ and τ_{Ee} can be derived to predict the performance of ohmically heated tokamak devices operated at very high densities.

V. ACKNOWLEDGMENTS

The authors thank the Alcator team for the pleasant cooperation during several periods; they are indebeted to Professors B. Coppi, R. R. Parker, and Dr. L. Th. M. Ornstein for stimulating discussions.

This work was performed under the Euratom-FOM association agreement with financial support from ZWO and Euratom and under the US-ERDA contract with MIT.

VI. REFERENCES

[1] Boxman, G. J. et al., Proc. 7th Eur. Conf. on Contr. Fusion and Plasma Phys., Lausanne (1975) II, 14.

[2] Apgar, E. et al., Proc. 6th Int. Conf. on Plasma Phys. and Contr. Nucl. Fusion Res., Berchtesgaden 1976, Suppl. to Nucl. Fusion (1977) Vol. 1, 247.

[3] Gandreau, M. et al., Phys. Rev. Lett. 39 (1977) 1266.

[4] Schram, D. C., Schüller, F. C. Rijnhuizen Report RR 77-104 (1977).

[5] Terry, J. L., et al., John Hopkins University, Baltimore, Maryland, USA, Technical Report No. COO-2711-3 (1977).

[6] Rutherford, P.M. et al., Proc. Int. Symp. on Plasma Wall Interaction, Jülich (1976) 173.

[7] Hazeltine, R. D., Hinton, F. L., Phys. Fluids, 16, 1883 (1973).

[8] Connor, J. W., Taylor, J. B., Culham Laboratory Report CLM-P485 (1977).